Multiple Guide Star Wavefront Sensing for Palomar AO

Venice 2001
Beyond Conventional Adaptive Optics

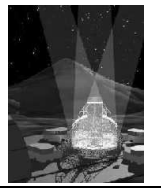

Richard Dekany,[a] Mitchell Troy,[b] Kent Wallace,[b]
Charlie Bleau,[c] Ray DuVarney,[c,d] and Garry Motter[c]

[a]California Institute of Technology, Pasadena, CA 91125 USA
[b]Jet Propulsion Laboratory, Pasadena, CA 91109 USA
[c]SciMeasure Analytical Systems, Inc., Atlanta, GA 30306 USA
[d]SciMeasure Analytical Systems, Inc., Atlanta, GA 30306 USA

ABSTRACT

Known single guide star techniques are insufficient to provide full-sky adaptive optics for extremely large telescopes. The use of multiple guide stars, either synthetic or natural, appears necessary, bringing new challenges in optical design, calibration, and operations. We present the design of a 4-channel Shack-Hartmann wavefront sensor under development at Caltech. Based upon a flexible, new high-speed camera architecture, this sensor will be used to conduct a set of multiple guide star experiments in conjunction with the existing adaptive optics system at the 5.1m diameter Hale Telescope at Palomar Mountain.

1. INTRODUCTION

Science with adaptive optics is currently limited by the availability of guide stars (Foy, 1985 and Rigaut, 1992) non-uniform point spread functions (Bloemhof, 2000), and small fields of view (Marshall, 2000). Through the use of laser guide stars, the first of these restrictions may be eased, with the cost of additional errors from Rayleigh pollution, tip-tilt indetermination (Pilkington, 1987), and focal anisoplanatism (Pilkington, 1987). The remaining two unsolved problems arise because, to date, astronomical adaptive optics has sought to solve a three-dimensional problem using two-dimensional sensing and correction techniques. Theoretically, all of these limitations can be removed by probing the three-dimensional structure of turbulence using multiple guide stars (Tallon, 1990, Murphy, 1991, and Ragazzoni, 1999) and correcting the atmospheric distortion using multiple deformable mirrors (Beckers, 1989).

We have begun a two-year project to build a multiple-guide-star wavefront sensing unit for use with the operational 241-actuator adaptive optics system (PALAO) at Palomar Mountain. This unit will enable simultaneous sampling and real-time recording of wavefront slope data from four different natural guide stars (NGS) by using four parallel Shack-Hartmann wavefront sensor channels. The products of this experiment are high frame rate wavefront slope data from which the status and evolution of the three-dimensional turbulence structure can be studied over a broad range of periods (from 10 millisecond scales up to seasonal variations). This information will be used in the design of future, more advanced adaptive optics systems in support of the envisioned 30 meter diameter California Extremely Large Telescope (CELT) (Nelson, 2000 and Dekany, 2000) adaptive optics needs.

2. ANISOPLANATISM WITHIN CLASSICAL ADAPTIVE OPTICS SYSTEMS

The details of turbulence in the Earth's atmosphere can have a profound effect on the quality of science obtainable with current adaptive optics systems. For purposes of discussion in this proposal, we take the point of view that the 3-D structure of turbulence can be approximated by a stratified set of discrete, thin phase layers, a position supported by experimental measurements (Rigaut, 1992).

Incident light from any two angularly separated points on the sky encounters different wavefronts during passage through the Earth's atmosphere. In Figure 1, we depict the optical path error imposed on light from each of two stars by two separate atmospheric layers, one at 10 km altitude described by an equivalent phase coherence diameter, $r_0(10\ km) = 0.11$ m and another at 0.5 km altitude described by $r_0(0.5\ km) = 0.26$ m (r_0 values are for 0.5μm wavelength). Below these, on axis, is the sum optical path difference encountered by an

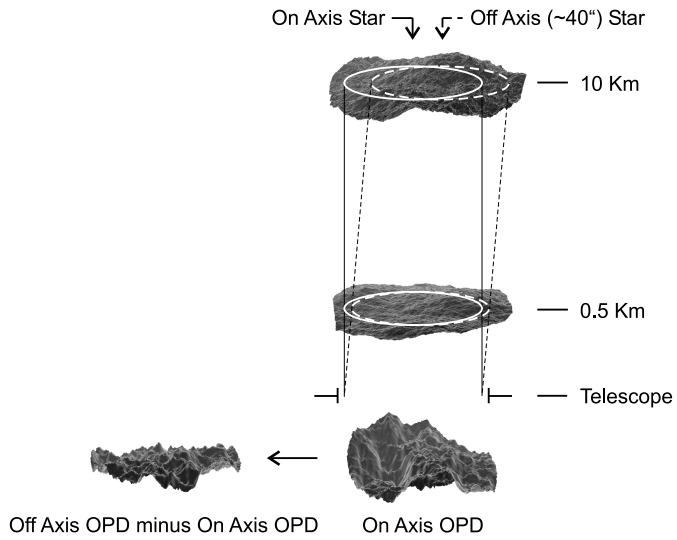

Figure 1. Representation of phase errors from two thin atmospheric layers, corresponding to $r_0(10\ km) = 0.11\ m$ and $r_0(0.5\ km) = 0.26\ m$. At bottom, the on-axis surface represents the sum wavefront, while the off-axis surface is the difference between the total off-axis and on-axis wavefronts. This figure quantitatively simulates a 5 m telescope with an on-axis and a 40 arcsecond off-axis star. The shear of the pupil at 10 km is 2 m, resulting in an rms phase difference of $\sim$ 600 nm (peak-to-valley 3.4μm) between the wavefronts seen by the two stars.

on-axis wavefront. Light originating from an off-axis source passes through a slanted path with respect to the on-axis star, and thus sees a different optical path. The residual error of applying the on-axis correction to an off-axis source is depicted by the lower surface, offset to the left.

The highly anisoplanatic angle on the right would pose a considerable challenge for accurate photometry. Our experience with PALAO is that often the anisoplanatic effects are consistent with a broadly distributed turbulence profile, although on occasion very wide uniformity of correction, as measured by fitted Strehl ratios, is observed (Marhsall, 2000). An example of measured anisoplanatism is presented in Figure 2. Note that the on-axis stars have FWHM's of 0.2 arcseconds and are symmetric while the stars at the edge of the field of view have FWHM's of 0.6 arcseconds and are elongated in one direction by 30%.

3. MULTIPLE GUIDE STAR EXPERIMENTAL INVESTIGATIONS

The multiple guide star unit (MGSU) being built PALAO will allow us to answer the following questions that cannot be conveniently or reliably explored through analysis or simulations:

- What is the structure and time evolution of the three-dimensional structure of atmospheric turbulence (as defined by $C_n^2(h,t)$)?
  - Kolmogorov / Rytov turbulence theory assumes an infinite atmosphere and does not account for variations in meterology and topography. Knowledge of the turbulence structure will allow understanding of energy cascades within the atmosphere, including factors driving the outer scale.
- To what extent can open-loop tomographic wavefront measurements be used for deconvolution of spatial varying point spread functions?
  - Adaptive optics has been implicitly based upon closed-loop operation of a wavefront sensor. Understanding the utility of open-loop wavefront sensor information may revolutionize approaches to adaptive optics, including the possibility of full-sky coverage on extremely large telescopes (Ragazzoni, 1999).
- To what extent can closed-loop adaptive correction, based upon tomographic information, increase the isoplanatic angle for imaging?

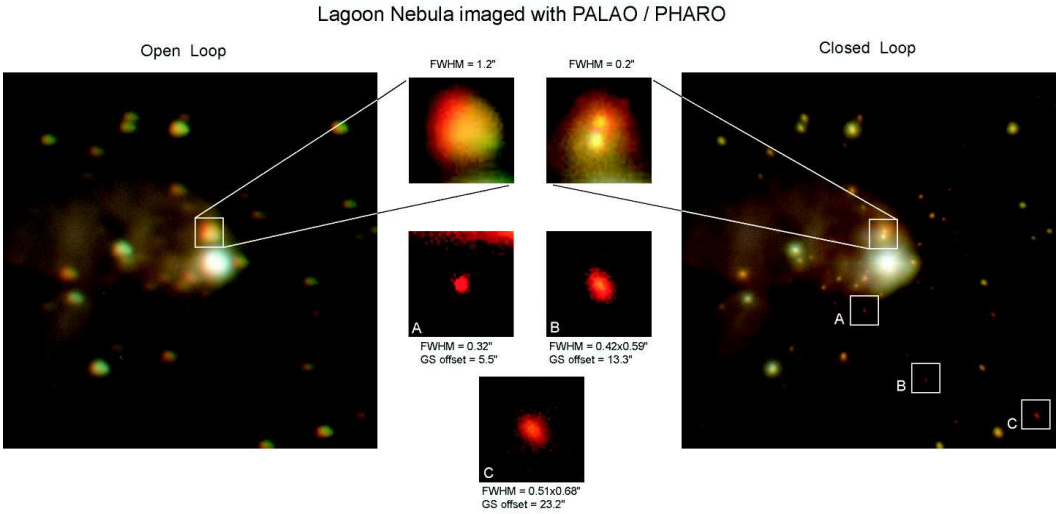

Figure 2. Thirty-second exposure open-loop (left) and closed-loop (right) J, H, K-band composite images of the Lagoon Nebula, M8, taken in poor conditions with the Palomar Adaptive Optics System and the Palomar High Angular Resolution Observer (Brandl, 1997). The top center two sub-images demonstrate the increase in resolving power provided by AO, while the lower three demonstrate the anisoplanacity of the AO corrected field. The K-band image FWHM falls from approximately 0.2 arcsec at the field center to greater then 0.6 arcsec at the edge of the 40 x 40 arcsec field of view.

  - Predictions of the utility of multiconjugate adaptive optics have varied widely (Fusco, 1999, Ellerbroek, 2000 and Ragazzoni, 2000) and only experimental investigation will determine the proper assumptions to incorporate into performance prediction models.

- Can low spatial frequency wavefront information from faint guide stars near the science object improve the wavefront estimate made using a bright, but more distant, guide star?

  - The density of natural guide stars increases very rapidly with diminishing brightness, making the availability of low spatial frequency wavefront information nearly certain. If this information can be used effectively, the general applicability of existing adaptive optics systems for extragalactic science could be increased significantly, with modest effort.

- What are the optimum trade-offs between multiple guide star geometry, brightness, and wavefront sensor camera integration times?

  - While the tradeoff between bandwidth and signal-to-noise ratio is understood for single guide star wavefront sensing, no one has considered the advantages of running multiple guide star wavefront sensors, in order to optimize the total information content.

- How valid is Taylor's frozen-flow hypothesis (Taylor, 1935) for atmospheric turbulence?

  - A quantitative determination of frozen-flow may open new possibilities for wavefront sensing techniques such as upstream point of laser guide stars, or more revolutionary ideas such as using farms of small telescopes surrounding future extremely large telescopes.

From these experiments we will make accurate predictions of the following:

- To what extent can tomographic wavefront information reduce conical anisoplanatism?

  - The residual errors arising from the finite altitude of laser guide stars (LGS) stands as a severe limitation to the performance of adaptive optics, particularly for extragalactic science. The use of tomographic estimation may remove this limitation.

- What are the optimum algorithms for combination of wavefront information from multiple laser guide stars?
  - The unique limitations on wavefront sensing with laser guide stars will likely lead to different techniques and algorithms than for natural guide star tomography. The combination of LGS and NGS information for optimal science performance is a further intellectual challenge that will be benefited from the proposed investigations.
- What are the practical limitations of laser guide star elongation on tomographic wavefront sensing?
  - Off-axis sensor elements suffer an additional wavefront error due to elongation of LGS spot in the sensor focal plane. To overcome conical anisoplanatism, many LGS, projected far off-axis, may be needed with large potential impact on laser power requirements.

Analytical and numerical simulations of alternative adaptive optics architectures for CELT will provide the context for our experimental investigations. The CELT AO design effort will utilize these results for model verification and to evaluate design trades and tolerancing levels for key subsystems

4. MEASUREMENT NOISE

In order to estimate the wavefront sensing capability of several natural guide star constellations, we consider the case of measurement noise within a Shack-Hartmann (SH) wavefront sensor. The rms wavefront error due to measurement uncertainty in the sensor (for $d > r_0$) is given by,

$$\sigma_{phase} = \frac{3\lambda d}{16 r_0 SNR} \tag{1}$$

where σ_{phase} is the wavefront uncertainty, λ is the WFS observing wavelength, r_0 is Fried's length, d is the subaperture width, and SNR is the signal-to-noise ratio per exposure per subaperture. In the case of high SNR (bright stars, photon noise limited), the measurement uncertainty is independent of subaperture diameter, while for low SNR (faint stars, read noise limited), the uncertainty is inversely proportional to the subaperture width, for a given brightness of guide star. We can then determine the brightness of guide star needed to obtain a given level of measurement tolerance, as shown in Figure 3. This chart shows the wavefront measurement uncertainty only. It is also informative to consider the effect of fitting error (Hardy, 1998)

$$\sigma_{fit} = \sqrt{0.17} \left(\frac{D}{r_0}\right)^{\frac{5}{6}} \left(\frac{\lambda}{2\pi}\right) [nm] \tag{2}$$

and error propagation in a slope sensor reconstructor (Hardy, 1998), both of which would be necessarily present in a real system based upon multiple SH wavefront sensors. The result of including these terms are shown in Figure 4. For large subapertures, the effect of fitting error is to prohibit low wavefront error levels (for any brightness of guide star).

5. MEASURING THE 3-D STRUCTURE OF ATMOSPHERIC TURBULENCE

By using multiple guide star signals to probe the structure of turbulence, it is possible to make an estimate of its three-dimensional structure at any given time (Angel, 2000). An estimate of the wavefront that has been parameterized by an ensemble of thin phase screens, can be derived from any number of wavefront sensor signals through a simple linear process,

$$e = My \tag{3}$$

where the phase estimate vector, e, is related to the wavefront sensor signal vector, y, through a reconstructor, M. The matrix M is a function of the vector angles describing the guide star geometry, the height distribution of turbulence, the turbulence power spectrum, the telescope diameter, the correcting element geometry and influence function, and noise in the sensor signal. The vector, y, is formed from the wavefront slope estimates from the four wavefront sensors. The matrix M is in general a function of time, making the accurate creation, calibration, and maintenance of $M(t)$ one of the primary objectives in understanding the potential utility of tomographic information on any future multiconjugate AO system (Ragazzoni, 1999 and Baharav, 1995). In

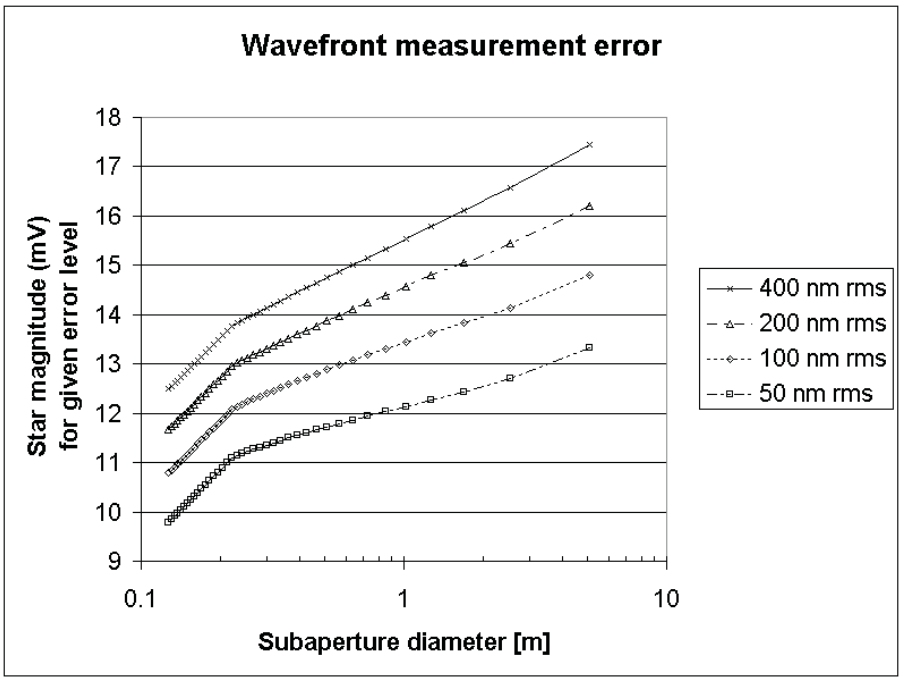

Figure 3. Measurement error vs. subaperture diameter, for $r_0(0.5mm) = 0.15\ m$, read noise = $3e^-$ rms, exposure time = 10 msec, system transmission = 0.36.

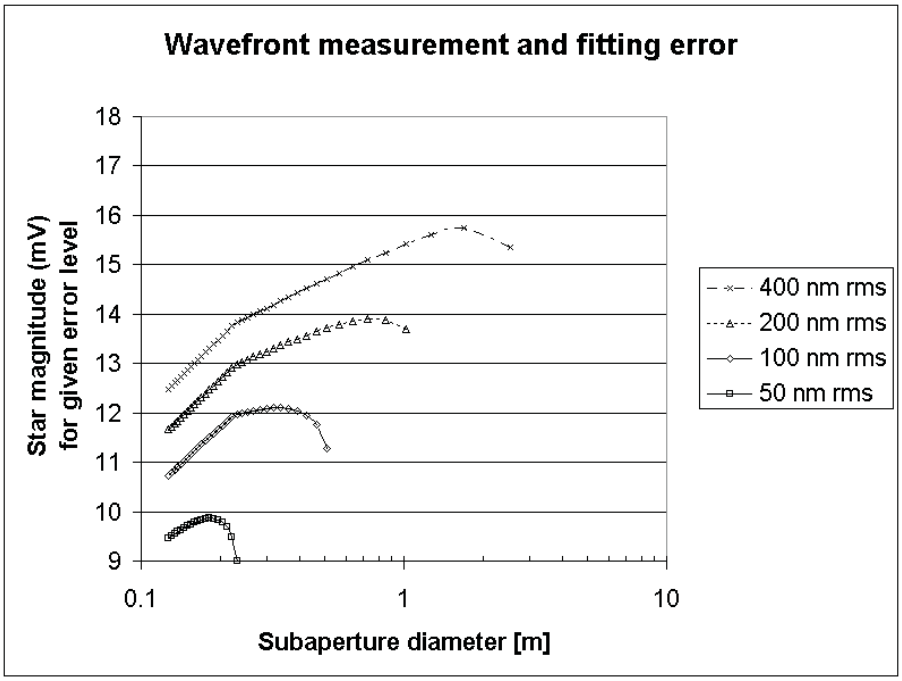

Figure 4. Combined measurement error and fitting error vs. subaperture diameter, for $r_0(0.5mm) = 0.15\ m$, read noise = $3e^-$ rms, exposure time = 10 msec, system transmission = 0.36. Each curve is truncated by the fitting error term, indicating that there is no brightness of star that results in that level of wavefront measurement error.

the case where read noise is not significant, which will be true in our initial experiments, the matrix M can be written as (Ragazzoni, 1999)

$$M = (AT^{+})^{+}L \tag{4}$$

where A is the geometry matrix of the actuators, T is a matrix which depends only on the turbulence as a function of height, $C_n^2(h)$, and L depends only the directions of the guide stars. An initial estimate of the matrix M can be computed explicitly using a package such as A++, which calculates optimum reconstructor matrix elements (Wild, 1998). Estimates of $C_n^2(h)$ can be calculated by correlating the slope maps obtained from the different guide stars. Since it is also possible to calculate the wind velocity as a function of height, which is needed for predictive control estimators, experimental verification of this technique is very important. Although promising results have been obtained using simulations, there is no substitute for direct measurements. The availability of the new wavefront sensor package is essential if new high performance AO techniques are to be developed by the community.

6. WFS CCD CAMERA ARCHITECTURE

PALAO currently uses a 64x64 MIT/LL CCD WFS camera built by SciMeasure Analytical Systems. Recently, a new controller has been built that has features particularly suitable for use in the MGSU, namely compact size and a more versatile data/telemetry interface. The architecture of the new controller has evolved over time and is based on the best parts of its predecessor, which has been described (DuVarney, 2000), but with several major conceptual changes that make it more flexible in its use, computer platform independent and expandable so as to handle a variety of CCDs with varying multiple port readouts. Photographs of new controller and an early version of the remote camera head are shown in Figures 5 and 6.

The camera head, which holds the CCD and the preamplifier, is remote from the controller electronics. This allows the small camera head (3" x 3" x 4") to be easily placed within a complex optical setup with minimal interference with the optical paths. The CCDs that are normally part of this head are usually cooled thermoelectrically. The waste heat, typically 10 watts, can be convectively and conductively removed with only a five degree centigrade rise in head temperature above ambient or alternatively fluid cooled with a negligibly small temperature rise. The preamplifier is customized for the CCD, conditions the clock and amplifies the signals to provide a uniform responsivity to the analog input modules.

The basic structure of the controller consists of a 3U height backplane and a series of five 100 x 160mm plug in modules which communicate with each other over that backplane and perform all the basic functions required for CCD control and readout. In addition to analog power and ground and the digital power and ground, the backplane carries the following signals: 24 bits of sequence data, up to 16 bits of digital data, a serial port communications bus, an I^2C bus and the 50 MHz system clock.

The most fundamental controller would consist of five modules:

The command module contains a RAM based sequencer and a microcontroller that handles communications over the serial port and over the I^2C bus. New sequences may be loaded into the sequencer via the serial link and this module also contains flash RAM to store a series of sequences that can, on command, be copied directly into sequence RAM. This module also supports a TTL level external hold command for the purposes of sequence synchronization. Using this feature, an external event such as a laser pulse could be used to begin the read out sequence. The sequencer would then return to the hold state or a hold sequence (such as integration) upon readout completion. In the case of the MGSU, the external hold mechanism will be used to synchronize several cameras to one master camera by using one or more bits from the sequencer in the master camera as the hold for the other cameras. In the hold state mode, synchronization can be accomplished to within 20 ns between master and slave cameras.

The clock driver module converts the TTL level clocking sequence information it receives over the backplane to driver level outputs that in turn exit the front of the module and go to the rear of the camera head. The clock hi and lo output levels on this module are adjustable between plus and minus 12 volts so long as the difference between them does not exceed 16 volts and overvoltage protection from this condition is contained in the module. One clock driver module can drive 15 outputs using 7 independent voltage hi and lo combinations.

The service module provides a suite of well-filtered adjustable bias voltages to operate the CCD. It also provides TEC cooling power and has 4 bias and 8-bit A/D circuits that provide internal case temperature, two

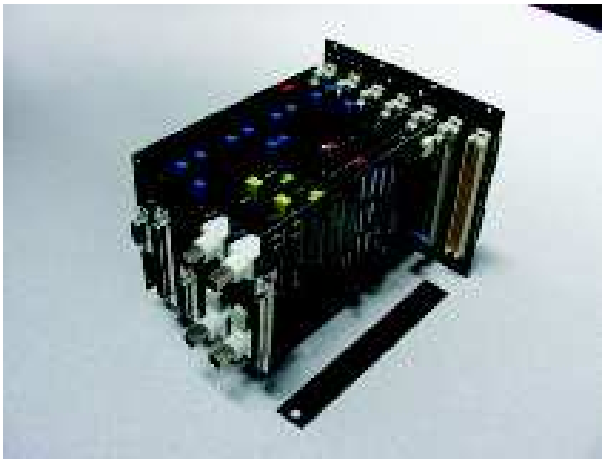

Figure 5. SciMeasure's new high-speed CCD camera controller.

CCD temperatures and vacuum information that is available over the I^2C bus. In addition, it can provide heater control through an 8-bit D/A circuit that is controlled through the I^2C bus.

The analog processing module contains two complete input processing channels each with four choices of gain and four choices of filter time constant. In addition, a high-speed filter bypass circuit is used, under sequence control, to greatly shorten the filter time constant to allow fast relaxation from events such as reset. The processing employs the Clamp and Sample methodology. Fine tuning of Clamp and Sample is possible via independently controllable 0.25 ns resolution delay lines, which is very useful in short sequences where the 20 ns system clock is too coarse. The Clamp levels for each channel are independently adjustable using a 10-bit DAC that is written to via the I^2C bus. The A to D converter, which resides at the end of the analog processing electronics, is built on a daughter card, making it relatively easy to switch from 12 to 14 to 16 bit resolution using the same analog processing module. This allows a trade-off between readout speed and dynamic range for a particular camera. In addition, each analog processing module has an identity selector between zero and seven. Thus on one backplane up to eight modules or sixteen channels of data can be simultaneously processed and sampled and the digital data multiplexed on the backplane's data bus. The multiplexed data is then available to the data output module which is described next.

One data output module receives the multiplexed data from the data bus and using start of line and start of frame commands, which are available on the backplane within the sequencer bus, puts the data into an AIA digital camera standard format. The module then transmits the data on differential drivers to the host computer, which contains one of many possible third party digital camera receivers supporting this AIA standard. The output module also implements the bidirectional serial port which is part of the definition of the AIA standard and thus supported by third party vendors supplying the receiver hardware and supporting device drivers for practically every platform and operating system.

The backplane is available in 7, 10, 15 and 21 slot versions, supporting a wide variety of configurations. For example, both the Marconi CCD39 and CCD50 would require a Command Module, a Clock Driver module, a Service Module, and a Data Output Module. However, the CCD39 (with four readout ports) requires 2 Analog Input Modules (a total of 6 modules) and the CCD50 (with 16 readout ports) requires 8 Analog Input Modules (a total of 12 modules). In addition, the backplane has an open specification that allows end users to customize the controller with their own modules such as Analog Input Modules, or Data Output Modules. Unused sequence bits are documented and can be used by end users for many kinds of functions requiring control that is synchronous with the readout.

The camera is controlled through an RS-232 serial port and is computer platform independent, but a GUI is provided, with source code, for Windows 32-bit operating systems. In addition, sequences can be written or customized for specific tasks using a simple language that includes Programs, Subroutines, Functions and Patterns, and a command line sequence compiler with source code is also provided.

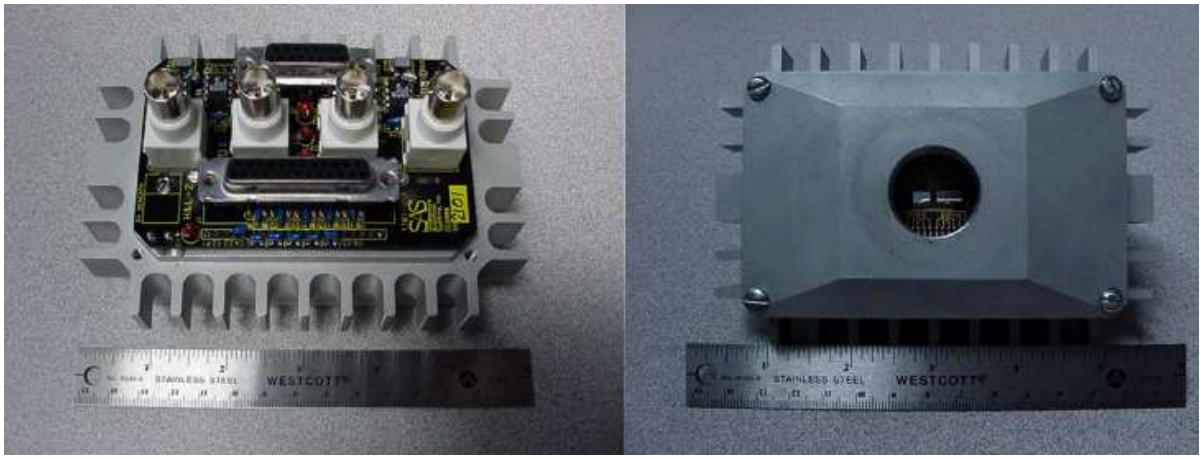

Figure 6. SciMeasure's new remote CCD camera head. This head may be located up to 8m away from the controller box in Figure 5, without measurable increase in camera noise.

7. THE MULTIPLE GUIDE STAR UNIT

The Multiple Guide Star Unit (MGSU) will architecturally consist of two arms, one that allows high-order wavefront sensing of up to four natural guide stars, which we are currently constructing, and a second arm dedicated to future wavefront sensing with laser guide stars.

The NGS arm of the MGSU consists of four Shack-Hartmann (SH) wavefront sensors, each capable of selecting one natural guide star from within a common 90" diameter field of view (FoV). Star selection is accomplished using small precision pick-off mirrors, as shown in Figure 7. Each pick off can span the entire field, but physical constraints set the nearest neighbor distance between stars to be approximately 5 arcseconds. Detailed optical design of the individual MGSU channels is currently in progress, and we expect to vary the number of SH subapertures for each channel

A partial layout of the MGSU, showing two of the four wavefront sensor channels is shown in Figure 7. In this picture, light from two stars is shown entering the MGSU from below, where each is pick off by a small fold mirror and fed to a Shack-Hartmann sensor arm that is rigidly integrated into the SciMeasure camera housing. Each arm/camera combination is placed onto a two-axis translation stage with travel sufficient to interrogate the entire 90" diameter unvignetted PALAO relay FoV.

The optomechanical integration of the MGSU into the existing PALAO system is currently under study. Initially, the MGSU will be used in conjuction with the existing SH-WFS (the 'master' WFS) which will continue to drive the adaptive correction of the AO loop. Thus, at first, the MGSU will be a 'spectator' that will measure anisoplanatic wavefront errors in the angular vicinity of the master guide star.

8. REAL-TIME TELEMETRY

We wish to record continuous Shack-Hartmann centroid information at a rate no less than 450 frames per second from all four camera channels. This requires the management of 1900 total frames per second. This represents a data stream of 1900 Hz x 512 centroids x 2 bytes $\sim$ 2 Mbyte/sec. In addition, we wish to record actuator and residual error signals, which results in an additional 900 Hz x 241 actuators x 2 signals x 2 bytes $\sim$ 1 Mbyte/sec stream. This represents an increased requirement over our current telemetry system, but not terribly so as broadband data architectures have similarly improved during the past several years.

9. FUTURE MULTI-CONJUGATE ADAPTIVE OPTICS AT PALOMAR

For our initial atmospheric experiments, we choose to employ Shack-Hartmann wavefront sensors for three reasons. First, the algorithms for SH wavefront reconstruction are well understood. Second, extensive experience in the practical use of SH-WFS's, including calibration techniques, has been gained with PALAO and other AO systems. Third, Palomar Observatory currently has at its disposal three fast frame-rate, low-noise cameras, developed by SciMeasureAnalytical Systems, Inc., that can be converted into SH use at minimum development cost. Details of these cameras capabilities are presented below. As progress in the field of large telescope

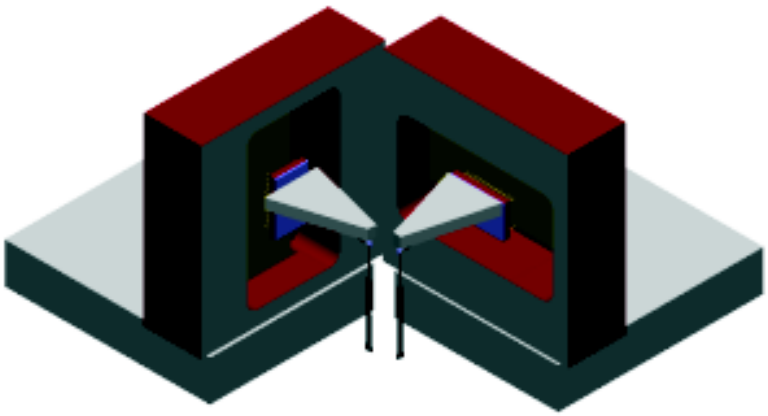

Figure 7. A depiction of two channels of the four-channel multiple guide star unit (MGSU). Incoming starlight is picked off by a small fold for each channel. The pickoff arms provide support for individual Shack-Hartmann relays (not shown) onto separate CCD detectors. Each of the 4 camera heads are symmetric, allowing 90 degree clocking (as shown), maintaining common pupil orientation on the sky. Each WFS camera is mounted on an x,y translation stage with 2 inch x 2 inch travel, allowing any WFS to interrogate the entire non-vignetted 90 arcsec diameter field of view of the PALAO system. Interference avoidance will ultimately by provided by software.

wavefront sensing is made, we envision these cameras as a flexible resource, if warranted, to explore alternative sensing techniques, such as curvature sensing (Roddier, 1991) or Foucault-like (pyramid) sensing (Riccardi, 1998) schemes.

In order to support proposed LGS experiments at Palomar Observatory, the MGSU would be upgraded with a LGS arm that would split the sodium wavelength light from the NGS light via a dichroic beamsplitter, prior to the field division. This would enable a new class of experiments, including the simultaneous sensing of multiple LGS and multiple NGS and the real-time correction of focal anisoplanatism.

We envision that, if the outcome of experiments described in this proposal support the utility of multiconjugate adaptive optics (MCAO), both the proposed NGS and future LGS arms of the MGSU will be used in a subsequent development phase to control multiple deformable mirrors in a closed-loop multiconjugate system. This stepwise approach reduces risk and allows us to concentrate on the unique problems of MCAO as they arise. Because our existing PHARO near-infrared science camera includes both imaging and R$\sim$ 1200 spectroscopic capability across J, H, and K bands, we will be prepared to take advantage of MCAO immediately. This is particularly true at J and H bands, where the isoplanatic angles, typically 8-16 arcsecs, limit the correction over PHARO's 25 and 40 arcsec square fields of view.

REFERENCES

Angel, J. R. P., Lloyd-Hart, M., "Atmospheric tomography with Rayleigh laser beacons for correction of wide fields and 30 m class telescopes", *Proc. SPIE*, **4003**, 270-276, (2000).

Baharav, Y., Shamir, J., "Increase in the compensated field of view with a double-conjugate adaptive-optics system", *Applied Optics*, **34**, 12, 2102-2110, (1995).

Beckers, J., M., *Proc. SPIE*, **1114**, 215-217, (1989).

Bloemhof, E. E., Marsh, K. A., Dekany, R. G., Troy, M., Marshall, J., Oppenheimer, B. R., "Stability of the adaptive-optic point-spread function: metrics, deconvolution, and initial Palomar results", *Proc. SPIE*, **4007**, (2000).

Brandl, B., Hayward, T. L., Houck, J. R., Gull, G. E., Pirger, B., Schoenwald, J., "PHARO (Palomar High Angular Resolution Observer) a dedicated NIR camera for the Palomar adaptive optics system", *Proc. SPIE*, **3126**, 515-521, (1997).

Dekany, R., Nelson, J. E., and Bauman, B., "Design considerations for CELT adaptive optics", *Proc. SPIE*, **4003**, (2000).

Ellerbroek, B., Rigaut, F., "Scaling Multiconjugate Adaptive Optics Performance Estimates to Extremely Large Telescopes", *Proc. SPIE*, **4003**, (2000).
Foy, R., Labeyrie, A., *Astron. Astrophys.*, **152**, L29-L31, (1985).
Fusco, T., Conan, J.-M., Michau, V., Mugnier, L. M., Rousset, G., "Phase estimation for large field of view: application to multiconjugate adaptive optics", *Proc. SPIE*, **3763**, 125-133, (1999).
Gardner, C. S., Welsh, B. M., Thompson, L. A., *IEEE Proc.*, **78**, 1721, (1990).
Hardy, J. W., *Adaptive Optics for Astronomical Telescopes*, Oxford Press, New York, (1998).
Marshall, J., Troy, M., Dekany, R. G., "Anisoplanicity studies within NGC6871", *Proc. SPIE*, **4007**, (2000).
Murphy, D., V., Primmermann, C. A., Zollars, B. G., Barclay, H. T., *Opt. Lett.*, **16**, 1797-1799, (1991).
Nelson, J. E., "Design Concepts for the California Extremely Large Telescope (CELT)", *Proc. SPIE*, **4004**, (2000).
Pilkington, J. D. H.,*Nature*, 320, 116, (1987).
Ragazzoni, R., Marchetti, E., Rigaut, F., "Modal tomography for adaptive optics", *Astron. Astrophys.*, **342**, L53-L56, (1999).
Ragazzoni, R., "No Laser Guide Stars for adaptive optics in giant telescopes?", *Astron. Astrophys. Suppl. Ser.*, **136**, 205-209, (1999).
Ragazzoni, R., Marchetti, E., and Valente, G., "Adaptive-optics corrections available for the whole sky", *Nature*, **403**, 54-56, (2000).
Rigaut, F., Gendron, E., *Astron. Astrophys.*, **261**, 677-684, (1992).
Rigaut, F., "Report on the Seeing on Mauna Kea" University of Hawaii, (1992).
Tallon, M., and Foy, R., *Astron. Astrophys.*, **235**, 549, (1990).
Taylor, G. I., "Statistical Theory of Turbulence", *Proceedings of the Royal Society*, **151**, 421-444, (1935).
Wild, W., J., "Innovative Wavefront Estimators for Zonal Adaptive Optics Systems. II", *Proc. SPIE*, **3353**, 1164-1173, (1998).